Stem Cell Research 43 (2020) 101698

Contents lists available at ScienceDirect

Stem Cell Research

journal homepage: www.elsevier.com/locate/scr

# Cryopreservation of human pluripotent stem cell-derived cardiomyocytes is not detrimental to their molecular and functional properties

Lettine van den Brink[a], Karina O. Brandão[a], Loukia Yiangou[a], Mervyn P.H. Mol[a], Catarina Grandela[a], Christine L. Mummery[a], Arie O. Verkerk[b], Richard P. Davis[a,*]

[a] Department of Anatomy and Embryology, Leiden University Medical Center, Einthovenweg 20, 2300 RC Leiden, the Netherlands
[b] Department of Medical Biology, Amsterdam UMC, 1105 AZ Amsterdam, the Netherlands

ARTICLE INFO

*Keywords:*
Human pluripotent stem cell-derived cardiomyocytes
Cryopreservation
Cardiac electrophysiology
Ventricular cardiomyocytes

ABSTRACT

Human induced pluripotent stem cell-derived cardiomyocytes (hiPSC-CMs) have emerged as a powerful platform for in vitro modelling of cardiac diseases, safety pharmacology and drug screening. All these applications require large quantities of well-characterised and standardised batches of hiPSC-CMs. Cryopreservation of hiPSC-CMs without affecting their biochemical or biophysical phenotype is essential for facilitating this, but ideally requires the cells being unchanged by the freeze-thaw procedure. We therefore compared the in vitro functional and molecular characteristics of fresh and cryopreserved hiPSC-CMs generated from multiple independent hiPSC lines. While the frozen hiPSC-CMs exhibited poorer replating than their freshly-derived counterparts, there was no difference in the proportion of cardiomyocytes retrieved from the mixed population when this was factored in, although for several lines a higher percentage of ventricular-like hiPSC-CMs were recovered following cryopreservation. Furthermore, cryopreserved hiPSC-CMs from one line exhibited longer action potential durations. These results provide evidence that cryopreservation does not compromise the in vitro molecular, physiological and mechanical properties of hiPSC-CMs, though can lead to an enrichment in ventricular myocytes. It also validates this procedure for storing hiPSC-CMs, thereby allowing the same batch of hiPSC-CMs to be used for multiple applications and evaluations.

## 1. Introduction

Human pluripotent stem cell-derived cardiomyocytes (hPSC-CMs) are now an established in vitro model and tool for studying cardiovascular development and disease, safety pharmacology and drug development, as well as having potential therapeutic applications (Brandão et al., 2017; Gerbin and Murry, 2015; Hartman et al., 2016; Magdy et al., 2018). Due to the significant progress made in efficiently differentiating hPSCs to cardiomyocytes, it is now possible to generate the large quantities of hPSC-CMs required for these purposes which can then be evaluated using a multitude of assays (Denning et al., 2016). To facilitate this, cryopreservation of hPSC-CMs is essential. Not only does the ability to freeze hPSC-CMs make the generation of these cells more cost and time effective, it also enables the same batch of hPSC-CMs to be analysed at multiple time points; thereby reducing this source of variability when performing multiple assays to investigate a disease phenotype or when carrying out large-scale drug discovery screens. From a clinical perspective, cryopreservation of the hPSC-CMs is also a necessary step to provide sufficient time to undertake quality control checks (Fujita and Zimmermann, 2018). Furthermore, cryopreservation allows the hPSC-CMs to be easily distributed among users, including to laboratories without the expertise or infrastructure to culture and differentiate hPSCs. Indeed, there are now several commercial suppliers that distribute cryopreserved hPSC-CMs for both academic and commercial applications (Blinova et al., 2018; Kitaguchi et al., 2016; Maddah et al., 2015).

Several reports have described procedures for freezing hPSC-CMs and using the resulting cryopreserved hPSC-CMs, for example in transplantation studies or for the generation of engineered heart tissue (Breckwoldt et al., 2017; Chong et al., 2014). While these protocols vary in the composition of the freezing medium, the majority include 10% dimethylsulfoxide (DMSO) as a cryoprotective agent and require the hPSC-CMs to be enzymatically dissociated into single cells. Obviously, it is critical that the cryopreservation procedure does not alter the molecular, biochemical or functional phenotype of the hPSC-CMs. While it has been demonstrated that frozen hPSC-CMs are viable upon thawing, express cardiac-specific markers, exhibit typical electrophysiological, calcium handling and contractility characteristics, and

* Corresponding author.
*E-mail address:* r.p.davis@lumc.nl (R.P. Davis).

https://doi.org/10.1016/j.scr.2019.101698
Received 29 June 2019; Received in revised form 6 December 2019; Accepted 30 December 2019
Available online 07 January 2020

can electrically couple in grafts (Blinova et al., 2018; Gerbin et al., 2015; Hwang et al., 2015; Kim et al., 2011; Puppala et al., 2013), these studies did not compare freshly-derived hPSC-CMs head-to-head with frozen-thawed batches. The few studies that have undertaken such a comparison have focussed on cardiomyocyte purity and viability immediately after thawing, as well as engraftment efficiency in rodents and non-human primates (Chen et al., 2015; Chong et al., 2014; Xu et al., 2011).

To date there have been no reports comparing the in vitro phenotype and physiological properties of cryopreserved and non-frozen hPSC-CMs following replating. Such studies are warranted due to the increasing use of hPSC-CMs for investigating disease mechanisms and in safety pharmacology assays (Denning et al., 2016; Giacomelli et al., 2017; van den Brink et al., 2019). For this reason, we have evaluated freshly-derived and cryopreserved cardiomyocytes generated from four different human induced pluripotent stem cell lines (hiPSC-CMs). The hiPSC-CMs were compared in terms of replating and cardiomyocyte subtype, as well as their electrophysiological and mechanical properties. Although the cryopreserved cells exhibited poorer replating efficiency after thawing, when this was sufficiently adjusted for, there was no difference in the proportion of cardiomyocytes recovered compared to the non-frozen cells. Intriguingly, for three hiPSC lines, cryopreservation resulted in an increased percentage of ventricular hiPSC-CMs, which was also reflected in a corresponding prolongation of the action potential (AP) duration for one of the cell lines. Furthermore, gene expression analysis of the cryopreserved hiPSC-CMs from this cell line indicated an upregulation of genes associated with a ventricular phenotype. Besides this, no other differences in the electrical and mechanical properties were observed, indicating that cryopreservation does not appear to be detrimental for the physiological attributes of hiPSC-CMs in vitro. As such, this study confirms that cryopreserved hiPSC-CMs retain their in vitro molecular and functional characteristics, and validates this as an opportune method for stockpiling hPSC-CMs for their use in downstream applications.

## 2. Results

### 2.1. Differentiation of hiPSCs to cardiomyocytes

The hiPSC lines, LUMC20 and LUMC99, were differentiated into cardiomyocytes, with spontaneously contracting regions typically observed around day 8 (d8) of differentiation (Fig. 1A and B). Both cell lines efficiently generated cardiomyocytes, with on average 82.7% ± 7.6% (LUMC20) and 86.5% ± 3.0% (LUMC99) of cells expressing the pan-cardiomyocyte marker cardiac troponin T (cTnT) at d21 of differentiation (Fig. 1C and D). At d21, the hiPSC-CMs were dissociated and either immediately replated (*fresh*) or cryopreserved for at least 7 days (on average 28 days). Cryopreservation was performed by a rate-controlled (−1 °C/min) temperature decrease to −80 °C in a freezing medium comprising 90% KnockOut Serum Replacement (KSR) and 10% DMSO. Non-frozen and thawed hiPSC-CMs from the same differentiation were compared under identical experimental conditions in terms of replating efficiency, cardiac marker expression and biophysical characteristics (AP and contraction).

### 2.2. Cryopreservation affects cell survival of replated cultures but not the relative hiPSC-CM contribution

To evaluate whether cryopreservation had any effect on cell viability, dissociated hiPSC-CMs were stained with trypan blue before and after freezing (Fig. 2A). There was no significant difference in the percentage of viable cells for LUMC20 (98.3 ± 0.3% non-frozen vs 95.7 ± 1.4% frozen, $p = 0.08$; unpaired *t*-test), indicating that the cryopreservation procedure did not cause significant necrosis. While cryopreserved hiPSC-CMs attached and expressed the cardiac markers α-actinin and myosin heavy chain (Fig. 2B), 24 h after replating the recovery of the cryopreserved cultures was approximately half that of their freshly replated counterparts ($15.5 \times 10^{-3} \pm 1.9 \times 10^{-3}$ A.U. non-frozen vs $9.2 \times 10^{-3} \pm 1.0 \times 10^{-3}$ A.U. frozen per $1.0 \times 10^{4}$ cells seeded) (Fig. 2C). This difference persisted for at least 7 days post-replating (Fig. 2C and D), suggesting that there was also no difference in proliferation rates between the differentiated cultures that were freshly replated or cryopreserved. Differences in replating efficiency were also observed for differentiated cells from LUMC99, with an approximately 3-fold poorer recovery for the cryopreserved hiPSC-CMs compared to the corresponding fresh cultures (Supplementary Fig. S1).

We therefore assessed whether this difference affected the proportion of hiPSC-CMs present in the replated cultures by flow cytometric analysis for cTnT, as well as the atrial and ventricular myosin light chain (MLC) isoforms (MLC2a and MLC2v respectively). The replating density did not appear to significantly affect the proportion of hiPSC-CMs that recovered when the cells were freshly replated (Supplementary Fig. S2). This is possibly due to the cardiomyocytes forming electrically-coupled clusters of cells that support their survival at low densities, leading to a web-like coverage and ultimately a sheet of contracting cells with few structural discontinuities at higher densities (Supplementary Fig. S3). Therefore, the non-frozen hiPSC-CMs were subsequently always seeded at $0.9 \times 10^{5}/cm^{2}$. However for the cryopreserved cells, higher seeding densities improved hiPSC-CM recovery based on the proportion of cells expressing cTnT (Supplementary Fig. S2C), resulting in similar percentages to that observed in the corresponding non-frozen hiPSC-CMs (Fig. 2E and F). Altering the seeding density also resulted in a corresponding increase in $MLC2a^{+}$ and $MLC2v^{+}$ cells (Fig. 2E and Supplementary Fig. S2C), although the overall percentage of hiPSC-CMs ($cTnT^{+}$ cells) expressing these markers did not vary between the different seeding densities (Fig. 2G). This indicated that while higher seeding densities improved the recovery of cryopreserved hiPSC-CMs, it did not influence the cardiomyocyte subtype or maturity.

We therefore factored in the difference in replating efficiency between the non-frozen and cryopreserved hiPSC-CMs by seeding approximately twice as many cryopreserved hiPSC-CMs per $cm^{2}$. We then observed no difference in the percentage of $cTnT^{+}$ hiPSC-CMs in the replated populations for the LUMC20 line (81.7 ± 4.9% non-frozen vs 81.3 ± 4.8% frozen) (Fig. 2H). However, for the LUMC99 line, the percentage of hiPSC-CMs recovered following cryopreservation still remained lower (69.8 ± 6.8% non-frozen vs 57.7 ± 8.1% frozen), possibly due to the less than 50% recovery of the replated frozen cells for this line (Supplementary Fig. S1B). Nonetheless, there was no difference in the proportion of hiPSC-CMs expressing MLC2a for either cell line (LUMC20, 81.1 ± 6.2% vs 82.7 ± 4.2%; LUMC99, 80.4 ± 4.3% vs 89.5 ± 4.5%; non-frozen vs frozen) (Fig. 2H). Additionally, we evaluated the effect of cryopreservation on cardiomyocytes generated from two hiPSC lines derived from hypertrophic cardiomyopathy (HCM) patients carrying a mutation in myosin binding protein C3 (Birket et al., 2015). Here too, similar percentages of $cTnT^{+}$ hiPSC-CMs were recovered between the fresh and frozen replated cells after compensating for the difference in the replating efficiency of the cryopreserved hiPSC-CMs (Supplementary Fig. S4A and B).

Interestingly, for LUMC20 and the two HCM lines, a greater proportion of the hiPSC-CMs expressed MLC2v following cryopreservation (LUMC20, 42.3 ± 6.6% vs 64.7 ± 6.0%; HCM1, 35.0% vs 57.3%; HCM3, 33.0 ± 11.8% vs 66.0 ± 9.8%; non-frozen vs frozen). While for LUMC99 a similar percentage of $MLC2v^{+}$ hiPSC-CMs were recovered upon thawing (36.0 ± 8.2% vs 38.8 ± 12.7%; non-frozen vs frozen) (Fig. 2H and Supplementary Fig. S4B). Although the percentage of $MLC2v^{+}$ hiPSC-CMs was variable between differentiations, it was almost always either higher or at a similar percentage in the cryopreserved hiPSC-CMs compared to the non-frozen counterpart (Supplementary Fig. S4C and D). Overall, these results suggest that, for some cell lines, cryopreservation might promote the maturation of hiPSC-CMs to a ventricular subtype. Prolonged storage of the hiPSC-CMs also

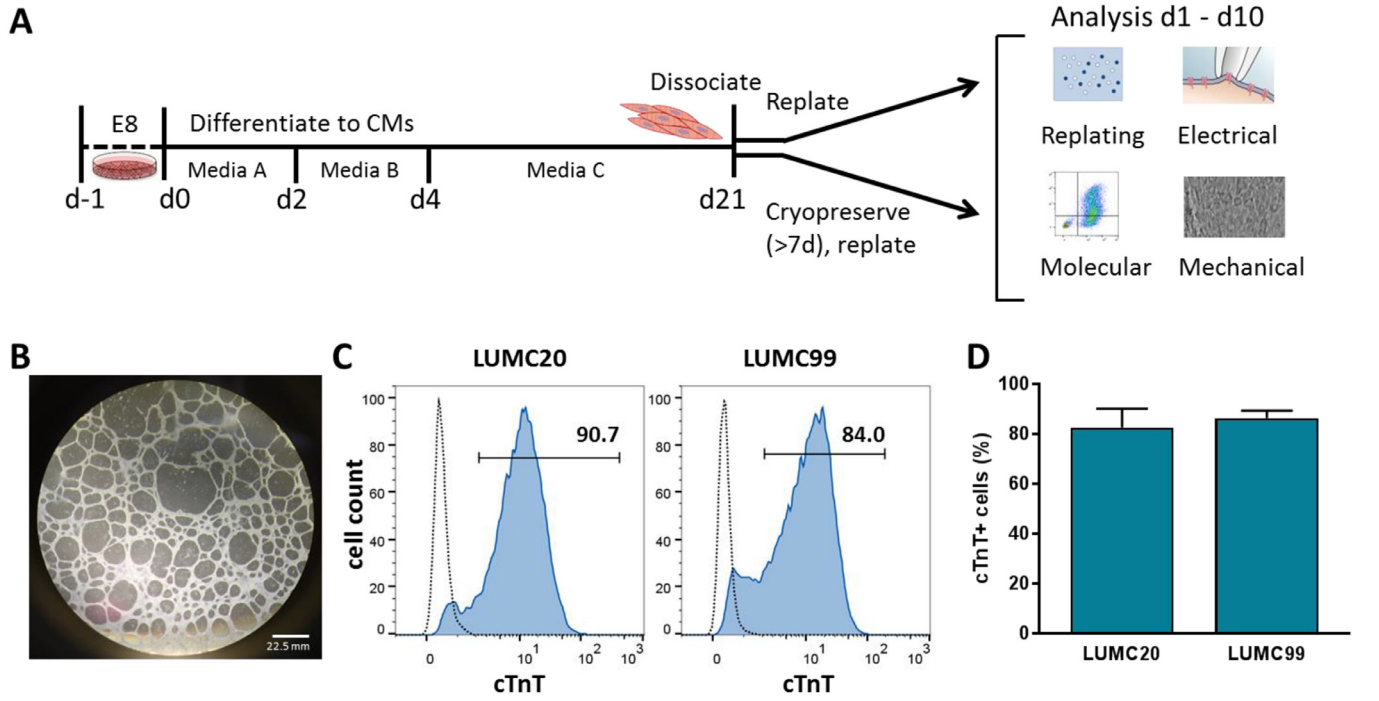


**Fig. 1.** Differentiation of hiPSC lines LUMC20 and LUMC99 to cardiomyocytes prior to cryopreservation and replating. A) Schematic outlining the differentiation procedure and subsequent analyses performed. At differentiation day (d)21, the dissociated hiPSC-CMs were either directly replated, or cryopreserved for at least 7 days before being thawed and replated. B) Phase-contrast image of a well containing d20 hiPSC-CMs derived from LUMC20. C) Representative histogram plots showing the percentage of $cTnT^+$ cells at d21 as determined by flow cytometry. Dotted lines represent a control $cTnT^-$ population. D) On average, for both LUMC20 and LUMC99, more than 80% of the cultures were cardiomyocytes as determined by flow cytometry analysis of cTnT ($n$ = 7 and 4 respectively).

did not affect expression of these cardiac markers, with the same batch of cells having similar values at both 1- and 8-months post-cryopreservation (Supplementary Fig. S5).

Finally, we also investigated the effect of cryopreservation on the expression of a panel of cardiac genes by qRT-PCR. When replated, both fresh and cryopreserved hiPSC-CMs derived from the LUMC20 line displayed gene expression changes associated with progression of heart development (Supplementary Fig. S6). This included the down-regulation of the fetal sarcomeric structural gene *MYH6*, and the up-regulation of the adult sarcomeric genes, *MYH7* and *TNNI3*. Furthermore, gene expression changes between the freshly replated and the frozen hiPSC-CMs corresponded to the flow cytometry data, with no difference in *TNNT2* expression detected, as well as upregulation of *MYL2* (the gene encoding for MLC2v) in hiPSC-CMs that had undergone a cryopreservation step (Fig. 2I). *MYL7* was also upregulated in the cryopreserved hiPSC-CMs, suggesting that additional post-transcriptional regulation of MLC2a expression occurred. There was also increased expression of ion channel genes involved in the cardiac AP (*SCN5A, KCNH2* and *KCNQ1*), upregulation of the $Ca^{2+}$-handling gene *PLN* (encoding phospholamban), as well as the sarcomeric assembly genes, *ACTN2* and *MYH7*. In addition, the cryopreserved hiPSC-CMs exhibited a higher *MYH7/MYH6* ratio when compared to the freshly replated hiPSC-CMs (Fig. 2J).

Taken together, these results indicated that while frozen hiPSC-CMs exhibited poorer replating efficiencies, cryopreservation did not significantly affect the proportion of hiPSC-CMs when this was correctly factored in after both short- and long-term storage. Furthermore, for some cell lines, this cryopreservation step significantly increased the proportion of hiPSC-CMs that attained a ventricular phenotype based on MLC2v expression at both an RNA and protein level. In addition, cryopreservation upregulated the expression of some genes associated with cardiac development, further indicating that cryopreservation does not harm the in vitro maturation of the hiPSC-CMs.

### 2.3. Cryopreservation is not detrimental to the electrical activity of hiPSC-CMs

Next, we performed AP measurements of fresh and cryopreserved hiPSC-CMs generated from the same differentiation. APs were recorded from single spontaneously contracting hiPSC-CMs and, to obtain a close-to-physiological resting membrane potential (RMP), we injected an in silico inward rectifier $K^+$ current ($I_{K1}$) with Kir2.1 characteristics using dynamic clamp methodology (Meijer van Putten et al., 2015). Fig. 3A shows representative APs from frozen and non-frozen cardiomyocytes derived from the two hiPSC lines, with average AP characteristics summarised in Fig. 3B (LUMC20) and Fig. 3C (LUMC99). Neither maximum AP upstroke velocity ($V_{max}$) nor AP amplitude (APA) showed significant differences between fresh and cryopreserved hiPSC-CMs from both hiPSC lines. The RMP as well as AP duration (APD) at 20, 50 and 90% repolarisation ($APD_{20}$, $APD_{50}$ and $APD_{90}$, respectively) were unaffected by cryopreservation for hiPSC-CMs derived from the LUMC99 hiPSC line (Fig. 3C). However, cryopreserved hiPSC-CMs from the LUMC20 hiPSC line showed a hyperpolarised RMP and prolonged APD (Fig. 3B). While differences in RMP might affect APDs by altering availability of sodium, calcium and potassium currents (Verkerk et al., 2017), we found no correlation between $APD_{90}$ and RMP (data not shown), suggesting that the longer APs in the frozen LUMC20 hiPSC-CMs may be due to the greater proportion of $MLC2v^+$ cardiomyocytes. Nevertheless, these results indicated that cryopreservation is not detrimental to the electrophysiological properties of the hiPSC-CMs in vitro.

### 2.4. Frozen and non-frozen hiPSC-CMs display similar contraction characteristics

Finally, we investigated whether cryopreservation affected the contractility of hiPSC-CMs relative to their fresh counterparts. Spontaneously contracting monolayers of hiPSC-CMs, as well as single

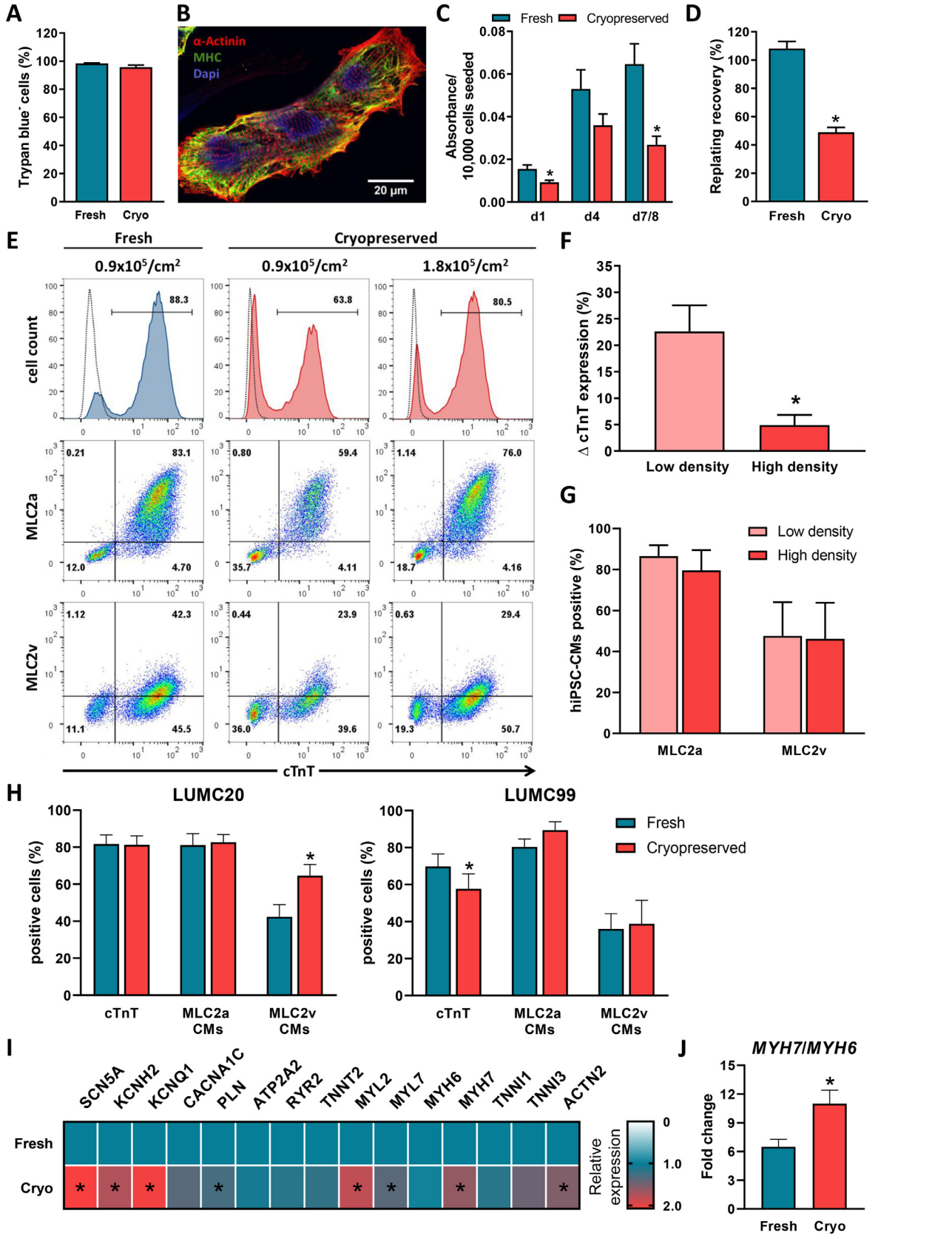


*(caption on next page)*

**Fig. 2.** Replating recovery and cardiac marker expression of non-frozen and cryopreserved hiPSC-CMs derived from LUMC20. A) Percentage of viable cells directly after dissociation (*fresh*) or upon thawing (*cryo*); $n = 14$ from 7 independent differentiations. B) Immunofluorescence image of cryopreserved hiPSC-CMs 6 days after thawing following staining with the sarcomere markers, α-actinin (red) and myosin heavy chain (MHC, green). Nuclei were stained with DAPI (blue). C) Recovery of fresh (blue) and cryopreserved (red) hiPSC-CMs (seeding density: 0.4–1.5 × $10^5$ cells/$cm^2$), at day 1, 4 and 7/8 post-replating. * indicates statistical significance (day 1 $p = 0.011$, day 7/8 $p = 0.007$, unpaired *t*-test); $n = 8$ from 4 independent differentiations. D) Percentage of replated fresh (blue) or cryopreserved (red) hiPSC-CMs recovered 7 days after seeding (seeding density: 0.5–2.6 × $10^5$ cells/$cm^2$), as determined by manual cell counting. * indicates statistical significance ($p < 0.0001$, unpaired *t*-test); $n = 12$ from 3 independent differentiations. E) Representative flow cytometric analysis of d21 + 7 hiPSC-CMs for expression of cTnT, MLC2a and MLC2v. Left column is non-frozen CMs, while the remaining columns are cryopreserved hiPSC-CMs plated at either the same density (0.9 × $10^5$/$cm^2$; *centre column*) or two-fold higher density (1.8 × $10^5$/$cm^2$; *right column*) as the non-frozen CMs. Top row depicts histogram plots of cTnT expression, while remaining rows depict bivariate density plots of MLC2a/cTnT (*middle row*) and MLC2v/cTnT (*bottom row*). Numbers inside the plots are percentage of cells within the gated region. Dotted lines represent a control $cTnT^-$ population. F) Bar graph showing difference (Δ) in cTnT expression compared to the corresponding fresh hiPSC-CMs when the cryopreserved hiPSC-CMs were seeded at low (0.9 × $10^5$/$cm^2$) or high (1.8–2.1 × $10^5$/$cm^2$) density. * indicates statistical significance ($p = 0.016$, unpaired *t*-test) ($n = 4$) G) Bar graph showing percentage of cryopreserved $cTnT^+$ hiPSC-CMs expressing MLC2a or MLC2v when seeded at either low (0.9 × $10^5$/$cm^2$) or high (1.8 × $10^5$/$cm^2$) density ($n = 4$) H) Bar graph showing percentage of freshly replated and cryopreserved cells expressing cTnT, as well as proportion of $cTnT^+$ hiPSC-CMs expressing MLC2a or MLC2v after taking into account differences in replating efficiencies for both LUMC20 (*left*) and LUMC99 (*right*) * indicates statistical significance (MLC2v CMs, $p = 0.015$; cTnT, $p = 0.03$, paired *t*-test); $n = 10$ (LUMC20) and $n = 6$ (LUMC99). I) Heat map showing changes in expression of key genes involved in the action potential, $Ca^{2+}$ regulation and sarcomere assembly of cardiomyocytes following cryopreservation of the hiPSC-CMs. Data is normalised to the housekeeping genes, *hARP* and *RLP37A,* and is relative to the expression levels in the freshly replated hiPSC-CMs. * indicates statistical significance (*ACTN2,* $p = 0007$; *KCNH2,* $p = 0.004$; *KCNQ1,* $p = 0.036$; *MYH7,* $p = 0.0001$; *MYL2, MYL7;* $p = 0.002$; *PLN,* $p = 0.008$; *SCN5A,* $p < 0.0001$, unpaired *t*-test); $n = 3$ independent differentiations. J) qRT-PCR analysis of the ratio of *MYH7/MYH6* expression in freshly replated and cryopreserved hiPSC-CMs. (For interpretation of the references to color in this figure legend, the reader is referred to the web version of this article.)

cells, were recorded with a high-sampling rate camera (100 fps) and analysed using the automated open source software tool MUSCLEMOTION (Sala et al., 2018). We chose to examine cardiomyocytes from the hiPSC line LUMC20 due to this line showing electrophysiological differences between the two groups. Representative contraction traces of fresh and cryopreserved hiPSC-CM monolayers paced at 1 Hz are shown in Fig. 4A, while the contraction parameters analysed are illustrated in Fig. 4B. Because the recordings of frozen and non-frozen hiPSC-CMs could not be made concurrently, exposure conditions varied thereby precluding the comparison of contraction amplitudes between the two groups. Therefore, contraction traces are presented with a contraction amplitude normalised to the maximal value.

Contraction duration at 90% peak amplitude (CD90), time-to-peak and relaxation time at day 3 and 7 post-replating were very similar between the fresh and cryopreserved cells in both hiPSC-CM monolayers and single cells (Fig. 4C and D). Congruently, no differences were observed for contraction duration (CD) at 10 and 50% peak amplitude (CD10 and CD50 respectively) values between the fresh and cryopreserved hiPSC-CMs (Supplementary Fig. S7A). Neither were differences detected when the fresh and cryopreserved hiPSC-CMs were stimulated at 2 Hz (Supplementary Fig. S7B-D). Overall these results indicated that cryopreservation does not affect the contractility of the hiPSC-CMs.

## 3. Discussion

Advances in hPSC-CM generation and phenotyping have made them valuable as in vitro models for studying human heart development and cardiovascular disease, as well as for cardiac safety pharmacology, drug screening and drug discovery (Brandão et al., 2017; Gerbin and Murry, 2015; Hartman et al., 2016; Magdy et al., 2018). While it is now possible to efficiently generate large quantities of relatively pure hPSC-CMs (Kempf and Zweigerdt, 2018), these procedures are time-consuming, laborious and are still subject to variability in reproducibility between successive differentiations (Burridge et al., 2015; Kempf et al., 2014). Efforts to cryopreserve hPSC-CMs have led to improved consistency in functional assays with comparable results obtained when the same batch of cells are used even between different laboratories (Hwang et al., 2015; Millard et al., 2018). However, evaluation of the effect of cryopreservation on the in vitro characteristics of the hPSC-CMs are limited. For example, previous studies have either only assessed the cryopreserved hPSC-CMs (Hwang et al., 2015; Kim et al., 2011; Puppala et al., 2013), or comparisons were performed on cells immediately before and after thawing without assessing the recovery of the culture (Chen et al., 2015). Here we have directly compared the phenotype and physiological properties of frozen and non-frozen hiPSC-CMs generated from the same differentiation experiment over a 10 day period post-replating. We have found that while cryopreservation can cause poorer replating of the hiPSC-CMs, this is not detrimental to their molecular, electrophysiological or contractile properties.

The (approximately two-fold) lower replating efficiency of the cryopreserved hiPSC-CMs compared to non-frozen cells is possibly due to cryoprotectant solution (90% KSR, 10% DMSO) or the freezing protocol (−1 °C/min to −80 °C) used in this study, and further optimisation of these steps would likely improve the recovery rate. Several other reports have used foetal bovine serum (FBS) instead of KSR (Hwang et al., 2015; Kim et al., 2011). We chose not to include animal serum since it is undefined, can show batch variability, and because all other maintenance and differentiation media used were serum-free. Other cryoprotectant solutions such as CryoStor CS-10 have also been used to cryopreserve hPSC-CMs (Chen et al., 2015; Xu et al., 2011); however we observed similar levels of recovery with this solution (data not shown). DMSO has been shown to be more cytotoxic to hiPSCs than other cryoprotective agents (Katkov et al., 2011), and so is also likely a cause of similar negative effects on hPSC-CMs. It is also apparent that the optimal cooling rate for cell survival varies depending on the cell type (Hunt, 2017). Therefore, further investigation of the most suitable cryoprotective agent and optimal cooling protocol for hPSC-CMs is warranted, in particular where these cells may be used therapeutically and large numbers of viable hPSC-CMs are required.

When the poorer replating efficiency of the cryopreserved hiPSC-CMs was adequately accounted for in the replating density, there was no difference in the proportion of cardiomyocytes recovered when compared to non-frozen hiPSC-CMs. The lower percentage of cardiomyocytes recovered following cryopreservation for LUMC99 was possibly due to the replating recovery being lower than the 50% value that was factored in. Interestingly, in three out four hiPSC lines, we observed a higher proportion of hiPSC-CMs expressing the ventricular marker MLC2v following cryopreservation. We further evaluated the effect of this on the cardiomyocytes derived from LUMC20. The cryopreserved hiPSC-CMs exhibited upregulated expression of several genes known to be highly expressed in ventricular cardiomyocytes, including *MYL2*, and an increased *MYH7/MYH6* ratio that is also associated with cardiac maturation (Veerman et al., 2015). Electrophysiologically, the cryopreserved cardiomyocytes from this line also displayed an increase in APD, as well as upregulated expression of ion channel genes involved in both phase 1 and 3 of the AP. These differences raise the possibility that cryopreservation could improve the maturation of the hPSC-CMs to a ventricular subtype.

A similar observation was evident in hPSC-CMs stored under hypothermic conditions (+4 °C), with the expression of several

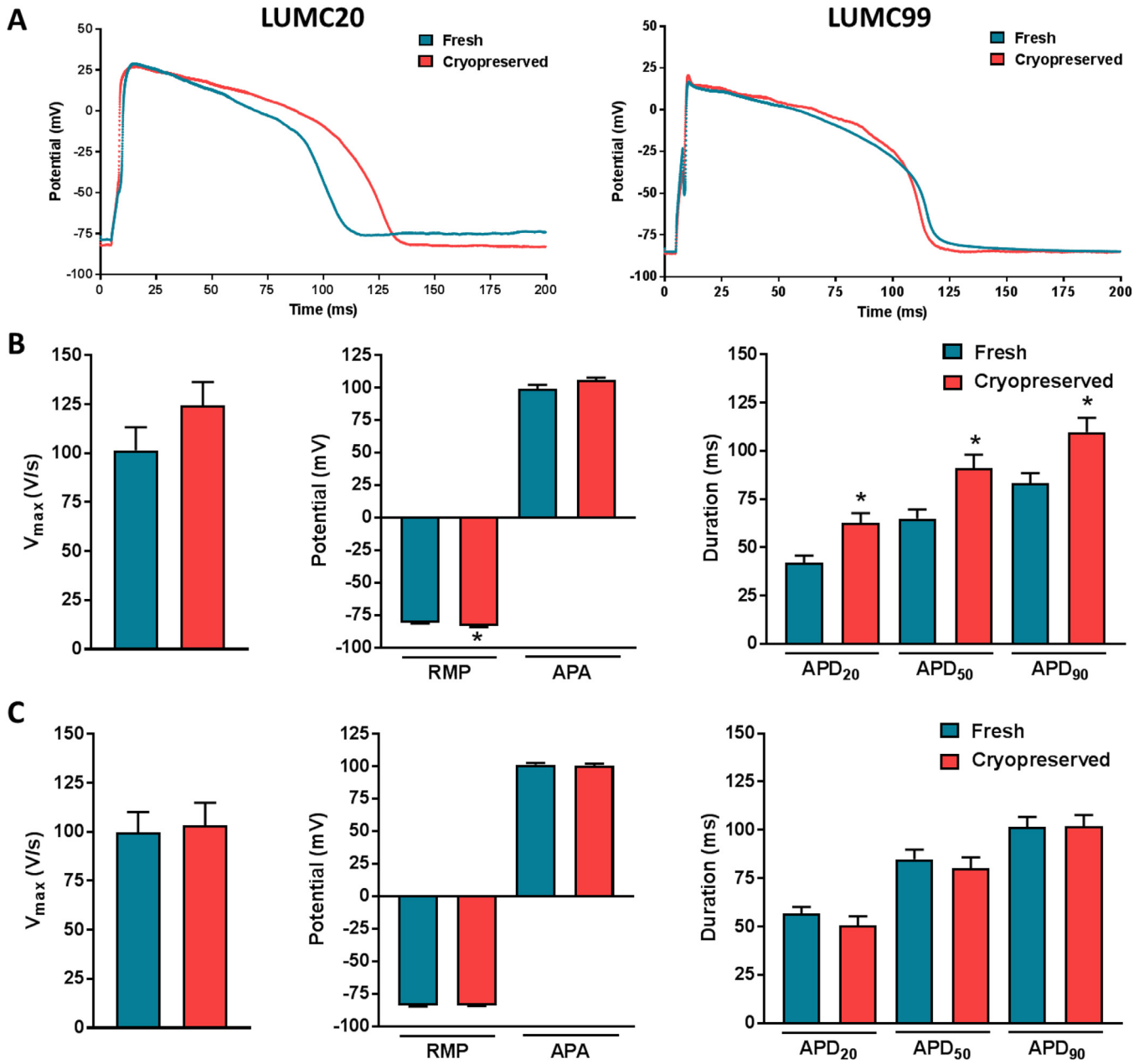


**Fig. 3.** Action potential (AP) characteristics of non-frozen and cryopreserved hiPSC-CMs. A) Representative AP traces of fresh and cryopreserved hiPSC-CMs measured at 1 Hz for both LUMC20 and LUMC99 cell lines. B & C) Average data at 1 Hz for maximal upstroke velocity ($V_{max}$), resting membrane potential (RMP), AP amplitude (APA) and AP duration at 20, 50, and 90% of repolarisation ($APD_{20}$, $APD_{50}$, and $APD_{90}$, respectively) for fresh and cryopreserved hiPSC-CMs for both LUMC20 (B) and LUMC99 (C) cell lines. For B, $n = 34$ and $n = 38$ respectively from 4 independent differentiations; for C, $n = 45$ and $n = 40$ respectively from 3 independent differentiations. * indicates statistical significance (RMP $p < 0.001$, $APD_{20}$ $p = 0.002$, $APD_{50}$ $p = 0.003$, $APD_{90}$ $p = 0.006$ unpaired *t*-test).

cardiomyocyte-specific genes including *MLC2v* significantly upregulated (Correia et al., 2016). The exact mechanism by which cold preservation could induce hPSC-CM maturation is unclear but hypothermic storage does increase caspase activity which has been demonstrated to promote the differentiation of mouse embryonic stem cell (ESC)-derived cardiac progenitors (Bulatovic et al., 2015). Alternatively, exposure of the hPSC-CMs to DMSO may also contribute to the enrichment in ventricular cardiomyocytes. Treatment of cultures with DMSO can downregulate *Oct-4* expression in mouse embryoid bodies as well as improve the differentiation of human ESC-derived pancreatic progenitors to terminal cell types (Adler et al., 2006; Chetty et al., 2013). In these studies, the concentration of DMSO was lower (<2% vs 10% in the cryoprotectant) but exposure was prolonged (1–2 days). Further studies are warranted to investigate whether cryopreservation or exposure of the hPSC-CMs to the cryoprotectant leads to enrichment of ventricular cardiomyocytes.

However, it should be noted that while the proportion of hiPSC-CMs we obtained between individual differentiations is quite consistent with the average percent of $cTnT^+$ cells being greater than 80%, we did observe some variability in the proportion of these cells that expressed MLC2v between different differentiations. It is possible that including an additional step in the differentiation procedure to direct the immature cardiomyocytes to a ventricular fate (Pei et al., 2017) could reduce this variability and would be worth further investigation. Regardless, we believe that it is prudent to also evaluate the percentage of $MLC2v^+$ hPSC-CMs when characterising batches to ensure that comparative functional assays are performed using differentiations containing similar proportions of ventricular cardiomyocytes.

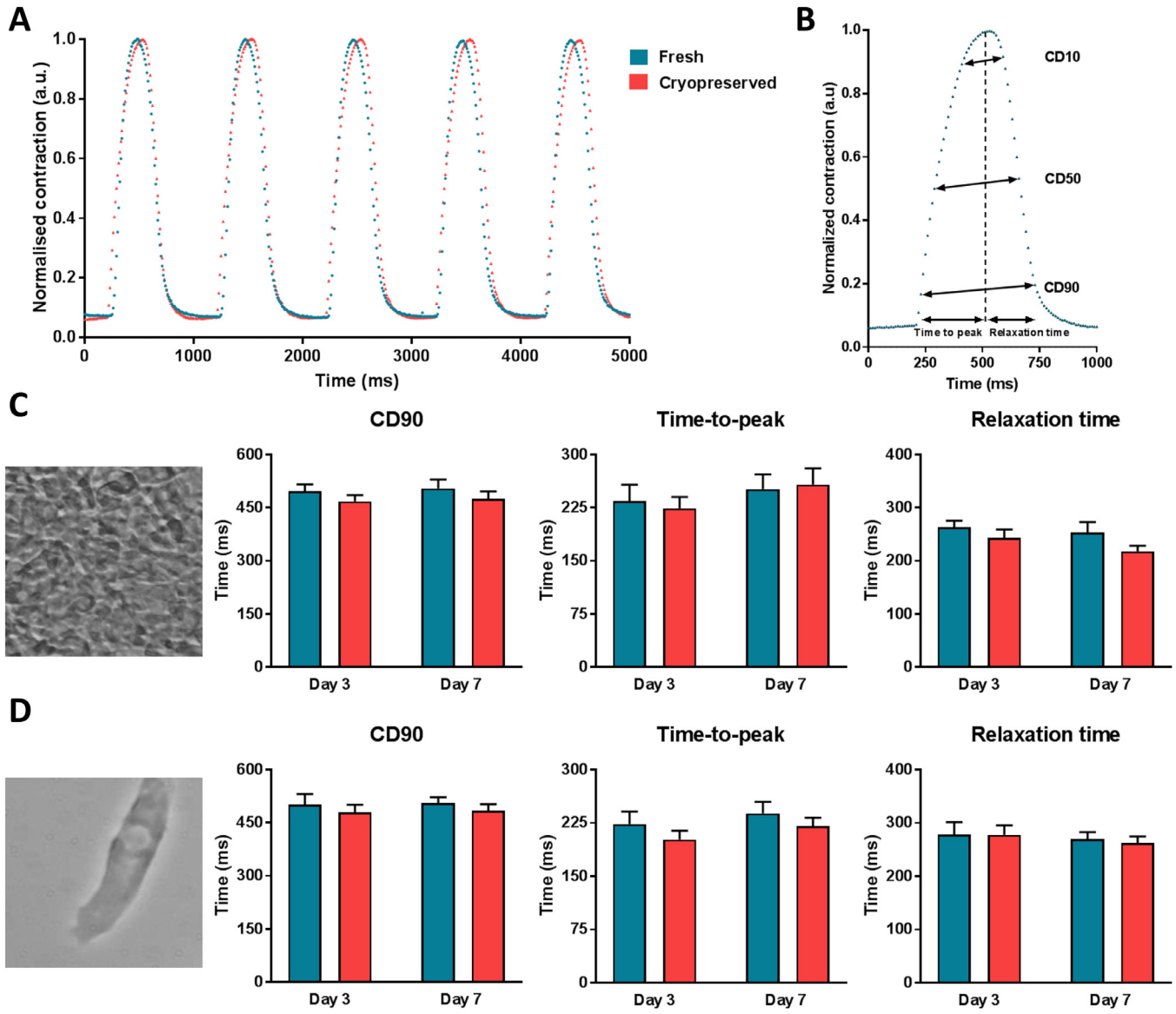


**Fig. 4.** Contraction characteristics of non-frozen and cryopreserved hiPSC-CMs. A) Representative normalised contraction traces measured at 1 Hz for fresh and cryopreserved LUMC20 hiPSC-CMs seeded as a monolayer. B) Contraction parameters measured from a normalised contraction trace. C & D) Average data at 1 Hz for contraction duration at 90% peak amplitude (CD90), time-to-peak and relaxation time for fresh and cryopreserved LUMC20 hiPSC-CMs measured in cells cultured either as monolayers (C) or single cells (D). Representative phase-contrast images are shown to the left of the bar graphs. For C, $n = 7$ and 9 (day 3); $n = 8$ and 9 (day 7) from 3 independent differentiations; For D, $n = 20$ and 30 (day 3); $n = 28$ and 28 (day 7) from 3 independent differentiations.

Importantly these results demonstrate that cryopreservation of hiPSC-CMs does not adversely affect their functionality. We believe this is the first reported head-to-head comparative study that has systematically quantified APs and contraction kinetics in non-frozen and frozen hiPSC-CMs obtained from the same differentiation. Although the electrophysiological characteristics of fresh and cryopreserved cardiomyocytes derived from the human ESC line H7 have been analysed (Peng et al., 2010; Xu et al., 2011), these studies were performed using different experimental conditions, including the age of the hPSC-CMs measured, composition of electrophysiological solutions, recording conditions and classification of the cardiomyocytes. Therefore, it remains unclear whether the prolonged $APD_{90}$ and slower $V_{max}$ observed in the frozen hPSC-CMs in these studies was due to the cryopreservation or experimental setup.

In conclusion, we have shown that apart from replating efficiency, cryopreservation is not detrimental to hiPSC-CMs. Further modifications of the cryoprotectant solution composition as well as the freezing and thawing process will likely further improve this. The ability to freeze and recover functional hPSC-CMs, along with recent advances in efficient differentiation of hPSCs to cardiomyocytes, will likely contribute to improvements in standardisation. Not only will this enable the same batch of hPSC-CMs to be used in multiple assays and thereby allowing more direct comparisons for cardiac disease modelling, it will also overcome some of the challenges in using hPSC-CMs for large-scale screening of pharmacological compounds. Finally, facilitating distribution of identical batches hPSC-CMs between laboratories might lead to improved experimental reliability and robustness, and contribute to addressing reproducibility issues in the field.

## 4. Material and methods

### 4.1. hiPSC-CM differentiation

Subclones from two control hiPSC lines (LUMC0020iCTRL (Zhang et al., 2014) [LUMC20]; LUMC0099iCTRL [LUMC99]), and two hiPSC lines derived from patients diagnosed with HCM

(LUMC0033iMyBPC [HCM1]; LUMC0035iMyBPC [HCM3] (Birket et al., 2015)) were maintained either in Essential 8 or StemFlex Medium (both Gibco). One day prior to differentiation (d-1), the hiPSCs were harvested using TrypLE Select (Gibco) and plated onto Matrigel-coated wells of a 12-well cell culture plate, either in Essential 8 Medium containing RevitaCell Supplement (1:200 dilution; Gibco) or StemFlex Medium at $3.9 \times 10^4/cm^2$. The hiPSCs were differentiated into cardiomyocytes either using the Pluricyte Cardiomyocyte Differentiation Kit (NCardia) according to the manufacturer's instructions, or in a modified BPEL medium (Elliott et al., 2011) supplemented with small molecules. Specifically, 5 μM CHIR99021 (Axon Medchem) from day 0 to day 2 of differentiation and 5 μM XAV939 + 0.25 μM IWP-L6 (AbMole) from differentiation day 2 to day 4. The hiPSC-CMs were maintained in Medium C (NCardia) until differentiation day 20–21 (LUMC20 and LUMC99), or the modified BPEL medium until differentiation day 14 or 17 (HCM1 and HCM3), and then dissociated as previously described (van den Berg et al., 2014).

### 4.2. hiPSC-CM cryopreservation, storage and thawing

The hiPSC-CMs were cryopreserved in a freezing medium comprising 90% KSR (Gibco) and 10% DMSO. Cryovials containing $\sim 1 \times 10^6$ cells in 300 μl freezing medium were rate-controlled (−1 °C/min) frozen to −80 °C. Approximately 24 h later, the vials were transferred and stored in liquid nitrogen (−196°C). For thawing, the vial was incubated at 37 °C and the thawed cells transferred to a conical tube. Immediately thereafter, 1 ml of BPEL medium (van den Berg et al., 2014) was added dropwise (1 drop every 5 s), followed by ~4.7 ml BPEL (1 drop every 2 s). Cell were precipitated at 250 g for 3 min and resuspended in Medium C.

### 4.3. Replating of hiPSC-CMs

Fresh and thawed hiPSC-CMs were replated on Matrigel-coated glass coverslips, or in 24-well cell culture plates in Medium C supplemented with RevitaCell Supplement (1:100 dilution) at the densities indicated. Approximately 24 h after plating the medium was refreshed, and subsequently every 2–3 days thereafter until the experiment was terminated.

### 4.4. Cell viability and replating efficiency

The viability of the dissociated hiPSC-CMs as well as the percentage of replated hiPSC-CMs recovered after 7 days was determined by trypan blue staining and manual counting using a hemocytometer. The viability and recovery of the replated cells was assessed at multiple time points using the CCK8 assay (Dojindo). For this, cells were seeded in multiple wells of a 24-well plate at varying densities ($0.4–1.5 \times 10^5/cm^2$). For each timepoint, the cell culture medium was removed and replaced with 330 μl of reaction mixture (300 μl Medium *C* + 30 μl CCK8 reagent) per well. After 2.5 h at 37°C, 100 μl from each well was transferred to a 96-well plate and the optical density (OD) at 450 nm measured using a Victor X3 microplate reader (Perkin Elmer). Reaction mixture added to a well without cells served as a blank control and was used to subtract the background fluorescence from the samples. The OD per $1 \times 10^4$ cells was then calculated. After measuring, the CCK8 treated-cells were washed twice with cell culture medium and replaced with Medium C.

### 4.5. Flow cytometry

Cells were plated in 24-well cell culture plates at densities between 0.9 and $2.1 \times 10^5/cm^2$. Approximately 7 days post-seeding, the cells were dissociated using TrypLE Select and filtered to remove cell aggregates. The cells were incubated with a Viobility™ 405/520 fixable dye (Miltenyi Biotech, Cat# 130-109-814) prior to fixation (FIX and PERM kit, Invitrogen) for subsequent exclusion of dead cells. Cells were co-labelled with cTnT (Vioblue-conjugated; Cat# 130-109-814), MLC2a (APC- or FITC-conjugated; Cat# 130-106-143 and 130-106-141 respectively) and MLC2v (PE-conjugated; Cat# 130-106-183) antibodies (all Miltenyi). All antibodies were used at a concentration of 1:11 in permeabilisation medium (medium B; Invitrogen). Data was acquired using a MacsQuant VYB flow cytometer (Miltenyi) and analysed with the software FlowJo (FlowJo, LLC).

### 4.6. Gene expression analysis

Total RNA was isolated from differentiated hiPSC-CMs at day 21 or from hiPSC-CMs replated at either $1.1 \times 10^5$ cells/$cm^2$ (fresh hiPSC-CMs) or $2.1 \times 10^5$ cells/$cm^2$ (cryopreserved hiPSC-CMs) using the Nucleospin RNA kit (Macherey-Nagel). Up to 1 μg of RNA for each sample was reverse transcribed using the iScript-cDNA Synthesis kit (Bio-Rad). Gene expression was assessed by qRT-PCR as described previously (Giacomelli et al., 2017a), with gene expression levels normalised to the reference genes, *RPL37A* and *HARP*. Primer sequences are provided in Supplementary Table S1.

### 4.7. Immunohistochemistry

The hiPSC-CMs were plated on glass coverslips at $0.7–1.3 \times 10^4/cm^2$ and fixed 6 days later using the Inside Stain Kit (Miltenyi) according to manufacturer's instructions. Fixed cells were incubated with α-actinin (1:250; Sigma; Cat# A7811) and myosin heavy chain (1:50; Miltenyi; Cat# 130-112-757) antibodies. The primary antibodies were detected with AF594- (1:200; Life Technologies; Cat# A-21203) and Vio515- (1:100; Miltenyi; Cat# 130-112-760) conjugated secondary antibodies, respectively. All antibodies were diluted in permeabilisation medium and incubated for 10 min. Cells were stained with 4′,6 Diamidino-2-Phenylindole (DAPI) (0.3 μM) for 5 min. Images were captured using a confocal laser scanning microscope SP8 (Leica).

### 4.8. Action potential measurements

The hiPSC-CMs were plated on 10 mm glass coverslips at $1.0 \times 10^4/cm^2$. APs were recorded 8–10 days later using the perforated patch-clamp technique and an Axopatch 200B amplifier (Molecular Devices). Single cells with spontaneous contractions (indicating the viable state of the cells) were selected. Using dynamic clamp, an in silico 2 pA/pF $I_{K1}$ with Kir2.1 characteristics was injected to obtain quiescent cells with a close-to-physiological RMP as previously described (Meijer van Putten et al., 2015). Data acquisition, voltage control and analysis was performed using custom made software, and the potentials were corrected for the calculated liquid junction potential (Barry and Lynch, 1991). The patch pipettes, estimations of cell membrane capacitance, filtering and digitising settings were as described previously (Verkerk et al., 2017).

Cells were superfused with modified Tyrode's solution (36 ± 0.2 °C) containing (in mM): 140 NaCl; 5.4 KCl; 1.8 $CaCl_2$; 1.0 $MgCl_2$; 5.5 glucose; 5.0 HEPES (pH 7.4; NaOH). Pipettes were filled with a solution containing (in mM): 125 K-gluconate; 20 KCl; 5.0 NaCl; 0.44 amphotericin-B; 10 HEPES (pH 7.2; KOH). APs were elicited at 1 Hz by 3 ms, ~1.2x threshold current pulses through the patch pipette, and analysed for RMP, $V_{max}$, APA, $APD_{20}$, $APD_{50}$ and $APD_{90}$. Parameters from 13 consecutive APs were averaged.

### 4.9. Contraction measurements

The contraction of single cells and monolayers of hiPSC-CMs was determined by seeding cells on 10 mm glass coverslips at a density of 1.0 or $12.7 \times 10^4/cm^2$ respectively. At day 3 and 7 post plating, coverslips were transferred into a bath superfused with modified Tyrode solution at 37°C. The single cells and monolayers were paced at 1 and

2 Hz using an external field stimulator. A 10 s movie was recorded using a DCC3240M camera (Thorlabs) with a sampling rate of 100 frames per second (fps). From the normalised contraction traces, the CD10, CD50, CD90, time-to-peak and relaxation time were calculated using the automated, open source software tool MUSCLEMOTION (Sala et al., 2018).

### 4.10. Statistical data analysis

All data are presented as mean ± SEM. Statistical tests performed are listed in the Results section or in the Fig. legends. Differences were considered statistically significant at $p < 0.05$. Analyses were conducted with Graphpad Prism 8 software.

## CRediT authorship contribution statement

**Lettine van den Brink:** Methodology, Investigation, Formal analysis, Writing - original draft, Writing - review & editing. **Karina O. Brandão:** Investigation. **Loukia Yiangou:** Investigation. **Mervyn P.H. Mol:** Investigation. **Catarina Grandela:** Investigation. **Christine L. Mummery:** Writing - review & editing. **Arie O. Verkerk:** Formal analysis, Writing - review & editing. **Richard P. Davis:** Conceptualization, Supervision, Formal analysis, Data curation, Writing - original draft, Writing - review & editing.

## Declaration of Competing Interest

C.L.M. is a cofounder of Pluriomics B.V. (now NCardia B.V.). All other authors declare no competing interests.

## Acknowledgments

We thank Leon Tertoolen and Berend van Meer for assistance with the MUSCLEMOTION software and Jelle Goeman for statistical advice. This work was supported by a Starting Grant (STEMCARDIORISK) from the European Research Council (ERC) under the European Union's Horizon 2020 Research and Innovation programme [H2020 European Research Council; grant agreement #638030], and a VIDI fellowship from the Netherlands Organisation for Scientific Research [Nederlandse Organisatie voor Wetenschappelijk Onderzoek; ILLUMINATE; #91715303].

## Supplementary materials

Supplementary material associated with this article can be found, in the online version, at doi:10.1016/j.scr.2019.101698.

## References

Adler, S., Pellizzer, C., Paparella, M., Hartung, T., Bremer, S., 2006. The effects of solvents on embryonic stem cell differentiation. Toxicol. Vitr. 20, 265–271.
Barry, P.H., Lynch, J.W., 1991. Liquid junction potentials and small cell effects in patch-clamp analysis. J. Membr. Biol. 121, 101–117.
Birket, M.J., Ribeiro, M.C., Kosmidis, G., Ward, D., Leitoguinho, A.R., van de Pol, V., Dambrot, C., Devalla, H.D., Davis, R.P., Mastroberardino, P.G., Atsma, D.E., Passier, R., Mummery, C.L., 2015. Contractile defect caused by mutation in MYBPC3 revealed under conditions optimized for human PSC-Cardiomyocyte function. Cell Rep. 13, 733–745.
Blinova, K., Dang, Q., Millard, D., Smith, G., Pierson, J., Guo, L., Brock, M., Lu, H.R., Kraushaar, U., Zeng, H., Shi, H., Zhang, X., Sawada, K., Osada, T., Kanda, Y., Sekino, Y., Pang, L., Feaster, T.K., Kettenhofen, R., Stockbridge, N., Strauss, D.G., Gintant, G., 2018. International multisite study of human-induced pluripotent stem cell-derived cardiomyocytes for drug proarrhythmic potential assessment. Cell Rep. 24, 3582–3592.
Brandão, K.O., Tabel, V.A., Atsma, D.E., Mummery, C.L., Davis, R.P., 2017. Human pluripotent stem cell models of cardiac disease: from mechanisms to therapies. Dis. Model. Mech. 10, 1039–1059.
Breckwoldt, K., Letuffe-Brenière, D., Mannhardt, I., Schulze, T., Ulmer, B., Werner, T., Benzin, A., Klampe, B., Reinsch, M.C., Laufer, S., Shibamiya, A., Prondzynski, M., Mearini, G., Schade, D., Fuchs, S., Neuber, C., Krämer, E., Saleem, U., Schulze, M.L., Rodriguez, M.L., Eschenhagen, T., Hansen, A., 2017. Differentiation of cardiomyocytes and generation of human engineered heart tissue. Nat. Protoc. 12, 1177–1197.
Bulatovic, I., Ibarra, C., Österholm, C., Wang, H., Beltrán-Rodríguez, A., Varas-Godoy, M., Månsson-Broberg, A., Uhlén, P., Simon, A., Grinnemo, K.-H., 2015. Sublethal caspase activation promotes generation of cardiomyocytes from embryonic stem cells. PLoS One 10, e0120176.
Burridge, P.W., Holmström, A., Wu, J.C., 2015. Chemically defined culture and cardiomyocyte differentiation of human pluripotent stem cells. Curr. Protoc. Hum. Genet. 87 21.3.1-21.3.15.
Chen, V.C., Ye, J., Shukla, P., Hua, G., Chen, D., Lin, Z., Liu, J.C., Chai, J., Gold, J., Wu, J., Hsu, D., Couture, L.A., 2015. Development of a scalable suspension culture for cardiac differentiation from human pluripotent stem cells. Stem Cell Res. 15, 365–375.
Chetty, S., Pagliuca, F.W., Honore, C., Kweudjeu, A., Rezania, A., Melton, D.A., 2013. A simple tool to improve pluripotent stem cell differentiation. Nat. Methods 10, 553–556.
Chong, J.J.H., Yang, X., Don, C.W., Minami, E., Liu, Y.W., Weyers, J.J., Mahoney, W.M., Van Biber, B., Cook, S.M., Palpant, N.J., Gantz, J.A., Fugate, J.A., Muskheli, V., Gough, G.M., Vogel, K.W., Astley, C.A., Hotchkiss, C.E., Baldessari, A., Pabon, L., Reinecke, H., Gill, E.A., Nelson, V., Kiem, H.P., Laflamme, M.A., Murry, C.E., 2014. Human embryonic-stem-cell-derived cardiomyocytes regenerate non-human primate hearts. Nature 510, 273–277.
Correia, C., Koshkin, A., Carido, M., Espinha, N., Šarić, T., Lima, P.A., Serra, M., Alves, P.M., 2016. Effective hypothermic storage of human pluripotent stem cell-derived cardiomyocytes compatible with global distribution of cells for clinical applications and toxicology testing. Stem Cells Transl. Med. 5, 658–669.
Denning, C., Borgdorff, V., Crutchley, J., Firth, K.S.A., George, V., Kalra, S., Kondrashov, A., Hoang, M.D., Mosqueira, D., Patel, A., Prodanov, L., Rajamohan, D., Skarnes, W.C., Smith, J.G.W., Young, L.E., 2016. Cardiomyocytes from human pluripotent stem cells: from laboratory curiosity to industrial biomedical platform. Biochim. Biophys. Acta 1863, 1728–1748.
Elliott, D.A., Braam, S.R., Koutsis, K., Ng, E.S., Jenny, R., Lagerqvist, E.L., Biben, C., Hatzistavrou, T., Hirst, C.E., Yu, Q.C., Skelton, R.J.P., Ward-Van Oostwaard, D., Lim, S.M., Khammy, O., Li, X., Hawes, S.M., Davis, R.P., Goulburn, A.L., Passier, R., Prall, O.W.J., Haynes, J.M., Pouton, C.W., Kaye, D.M., Mummery, C.L., Elefanty, A.G., Stanley, E.G., 2011. NKX2-5 eGFP/w hESCs for isolation of human cardiac progenitors and cardiomyocytes. Nat. Methods 8, 1037–1043.
Fujita, B., Zimmermann, W.-H., 2018. Myocardial tissue engineering strategies for heart repair: current state of the art. Interact. Cardiovasc. Thorac. Surg. 27, 916–920.
Gerbin, K.A., Murry, C.E., 2015. The winding road to regenerating the human heart. Cardiovasc. Pathol. 24, 133–140.
Gerbin, K.A., Yang, X., Murry, C.E., Coulombe, K.L.K., 2015. Enhanced electrical integration of engineered human myocardium via intramyocardial versus epicardial delivery in infarcted rat hearts. PLoS One 10, e0131446.
Giacomelli, E., Bellin, M., Sala, L., van Meer, B.J., Tertoolen, L.G.J., Orlova, V.V., Mummery, C.L., 2017a. Three-dimensional cardiac microtissues composed of cardiomyocytes and endothelial cells co-differentiated from human pluripotent stem cells. Development 144, 1008–1017.
Giacomelli, E., Mummery, C.L., Bellin, M., 2017b. Human heart disease: lessons from human pluripotent stem cell-derived cardiomyocytes. Cell. Mol. Life Sci. 74, 3711–3739.
Hartman, M.E., Dai, D.-F., Laflamme, M.A., 2016. Human pluripotent stem cells: prospects and challenges as a source of cardiomyocytes for in vitro modeling and cell-based cardiac repair. Adv. Drug Deliv. Rev. 96, 3–17.
Hunt, C.J., 2017. Cryopreservation: vitrification and controlled rate cooling. Methods Mol. Biol. 1590, 41–77.
Hwang, H.S., Kryshtal, D.O., Feaster, T.K., Sánchez-Freire, V., Zhang, J., Kamp, T.J., Hong, C.C., Wu, J.C., Knollmann, B.C., 2015. Comparable calcium handling of human iPSC-derived cardiomyocytes generated by multiple laboratories. J. Mol. Cell. Cardiol. 85, 79–88.
Katkov, I.I., Kan, N.G., Cimadamore, F., Nelson, B., Snyder, E.Y., Terskikh, A.V., 2011. DMSO-free programmed cryopreservation of fully dissociated and adherent human induced pluripotent stem cells. Stem Cells Int. 2011, 981606.
Kempf, H., Olmer, R., Kropp, C., Rückert, M., Jara-Avaca, M., Robles-Diaz, D., Franke, A., Elliott, D.A., Wojciechowski, D., Fischer, M., Roa Lara, A., Kensah, G., Gruh, I., Haverich, A., Martin, U., Zweigerdt, R., 2014. Controlling expansion and cardiomyogenic differentiation of human pluripotent stem cells in scalable suspension culture. Stem Cell Rep. 3, 1132–1146.
Kempf, H., Zweigerdt, R., 2018. Scalable cardiac differentiation of pluripotent stem cells using specific growth factors and small molecules. Adv. Biochem. Eng. Biotechnol. 163, 39–69.
Kim, Y.Y., Ku, S.Y., Liu, H.C., Cho, H.J., Oh, S.K., Moon, S.Y., Choi, Y.M., 2011. Cryopreservation of human embryonic stem cells derived-cardiomyocytes induced by BMP2 in serum-free condition. Reprod. Sci. 18, 252–260.
Kitaguchi, T., Moriyama, Y., Taniguchi, T., Ojima, A., Ando, H., Uda, T., Otabe, K., Oguchi, M., Shimizu, S., Saito, H., Morita, M., Toratani, A., Asayama, M., Yamamoto, W., Matsumoto, E., Saji, D., Ohnaka, H., Tanaka, K., Washio, I., Miyamoto, N., 2016. CSAHi study: evaluation of multi-electrode array in combination with human iPS cell-derived cardiomyocytes to predict drug-induced QT prolongation and arrhythmia-effects of 7 reference compounds at 10 facilities. J. Pharmacol. Toxicol. Methods 78, 93–102.
Maddah, M., Heidmann, J.D., Mandegar, M.A., Walker, C.D., Bolouki, S., Conklin, B.R., Loewke, K.E., 2015. A non-invasive platform for functional characterization of stem-cell-derived cardiomyocytes with applications in cardiotoxicity testing. Stem Cell Rep. 4, 621–631.
Magdy, T., Schuldt, A.J.T., Wu, J.C., Bernstein, D., Burridge, P.W., 2018. Human induced pluripotent stem cell (hiPSC)-derived cells to assess drug cardiotoxicity: opportunities

and problems. Annu. Rev. Pharmacol. Toxicol. 58, 83–103.
Meijer van Putten, R.M.E., Mengarelli, I., Guan, K., Zegers, J.G., van Ginneken, A.C.G., Verkerk, A.O., Wilders, R., 2015. Ion channelopathies in human induced pluripotent stem cell derived cardiomyocytes: a dynamic clamp study with virtual IK1. Front. Physiol. 6, 7.
Millard, D., Dang, Q., Shi, H., Zhang, X., Strock, C., Kraushaar, U., Zeng, H., Levesque, P., Lu, H.R., Guillon, J.M., Wu, J.C., Li, Y., Luerman, G., Anson, B., Guo, L., Clements, M., Abassi, Y.A., Ross, J., Pierson, J., Gintant, G., 2018. Cross-site reliability of human induced pluripotent stem cell-derived cardiomyocyte based safety assays using microelectrode arrays: results from a blinded CIPA pilot study. Toxicol. Sci. 164, 550–562.
Pei, F., Jiang, J., Bai, S., Cao, H., Tian, L., Zhao, Y., Yang, C., Dong, H., Ma, Y., 2017. Chemical-defined and albumin-free generation of human atrial and ventricular myocytes from human pluripotent stem cells. Stem Cell Res. 19, 94–103.
Peng, S., Lacerda, A.E., Kirsch, G.E., Brown, A.M., Bruening-Wright, A., 2010. The action potential and comparative pharmacology of stem cell-derived human cardiomyocytes. J. Pharmacol. Toxicol. Methods 61, 277–286.
Puppala, D., Collis, L.P., Sun, S.Z., Bonato, V., Chen, X., Anson, B., Pletcher, M., Fermini, B., Engle, S.J., 2013. Comparative gene expression profiling in human-induced pluripotent stem cell-derived cardiocytes and human and cynomolgus heart tissue. Toxicol. Sci. 131, 292–301.
Sala, L., Van Meer, B.J., Tertoolen, L.G.J., Bakkers, J., Bellin, M., Davis, R.P., Denning, C., Dieben, M.A.E., Eschenhagen, T., Giacomelli, E., Grandela, C., Hansen, A., Holman, E.R., Jongbloed, M.R.M., Kamel, S.M., Koopman, C.D., Lachaud, Q., Mannhardt, I., Mol, M.P.H., Mosqueira, D., Orlova, V.V., Passier, R., Ribeiro, M.C., Saleem, U., Smith, G.L., Burton, F.L., Mummery, C.L., 2018. Musclemotion: a versatile open software tool to quantify cardiomyocyte and cardiac muscle contraction in vitro and in vivo. Circ. Res. 122, e5–e16.
van den Berg, C.W., Elliott, D.A., Braam, S.R., Mummery, C.L., Davis, R.P., 2014. Differentiation of human pluripotent stem cells to cardiomyocytes under defined conditions. Methods Mol. Biol. 1353, 163–180.
van den Brink, L., Grandela, C., Mummery, C.L., Davis, R.P., 2019. Inherited cardiac diseases, pluripotent stem cells, and genome editing combined - the past, present, and future. Stem Cells. https://doi.org/10.1002/stem.3110. In press.
Veerman, C.C., Kosmidis, G., Mummery, C.L., Casini, S., Verkerk, A.O., Bellin, M., 2015. Immaturity of human stem-cell-derived cardiomyocytes in culture: fatal flaw or soluble problem? Stem Cells Dev. 24, 1035–1052.
Verkerk, A.O., Veerman, C.C., Zegers, J.G., Mengarelli, I., Bezzina, C.R., Wilders, R., 2017. Patch-clamp recording from human induced pluripotent stem cell-derived cardiomyocytes: improving action potential characteristics throughdynamic clamp. Int. J. Mol. Sci. 18, 1873.
Xu, C., Police, S., Hassanipour, M., Li, Y., Chen, Y., Priest, C., O'Sullivan, C., Laflamme, M.A., Zhu, W.-Z., Van Biber, B., Hegerova, L., Yang, J., Delavan-Boorsma, K., Davies, A., Lebkowski, J., Gold, J.D., 2011. Efficient generation and cryopreservation of cardiomyocytes derived from human embryonic stem cells. Regen. Med. 6, 53–66.
Zhang, M., D'Aniello, C., Verkerk, A.O., Wrobel, E., Frank, S., Ward-van Oostwaard, D., Piccini, I., Freund, C., Rao, J., Seebohm, G., Atsma, D.E., Schulze-Bahr, E., Mummery, C.L., Greber, B., Bellin, M., 2014. Recessive cardiac phenotypes in induced pluripotent stem cell models of Jervell and Lange-Nielsen syndrome: disease mechanisms and pharmacological rescue. Proc. Natl. Acad. Sci. USA 111, E5383–E5392.